JOURNAL OF CATALYSIS 157, 512–522 (1995)

Step and Pulse Transient Studies of IR-Observable Adsorbates during NO and CO Reaction on Rh/SiO_2

Raja Krishnamurthy,[1] Steven S. C. Chuang,[2] and Michael W. Balakos[3]

Department of Chemical Engineering, The University of Akron, Akron, Ohio 44325-3906

Received November 21, 1994; revised June 15, 1995; accepted July 18, 1995

The dynamics and reactivity of infrared-observable adsorbates for the reaction of NO with CO over a 44% Rh/SiO_2 catalyst have been studied by *in situ* infrared spectroscopy combined with steady-state isotopic and pulse NO–CO transient techniques. Steady-state isotopic transient results reveal that (i) a rapid exchange between the gaseous CO and adsorbed CO occurs on the Rh surface; (ii) $Rh^+(^{12}CO)(^{13}CO)$ is an intermediate for the exchange between $Rh^+(^{12}CO)_2$ and gaseous ^{13}CO; (iii) the adsorbed NCO species is not directly involved in the formation of CO_2; (iv) the residence time of the intermediate for CO_2 formation decreases with an increase in temperature from 473 to 573 K. At 573 K, rapid NO dissociation led to the high availability of surface oxygen, which results in CO_2 response leading the CO response during steady-state isotopic transient studies. Pulse NO–CO transients further confirm that the NCO species is not a reaction intermediate in the formation of CO_2. Pulse NO–CO studies show that Rh–NO^-, Rh–NCO, and CO_2 are formed prior to gem-dicarbonyl; CO_2 can be produced without involving the gem-dicarbonyl as an intermediate. Steady-state isotopic transient and pulse studies were excellent complementary techniques that provided an insight into the reactivity and dynamics of adsorbates under reaction condition.

INTRODUCTION

The catalytic reaction of NO with CO to form N_2 and CO_2 is an important subject in environmental catalysis (1–8). Several studies have suggested that CO_2 is formed from the reaction of adsorbed CO with adsorbed oxygen produced from the dissociation of adsorbed NO on the metal surface (2–9). CO can chemisorb in the linear, bridged, and gem-dicarbonyl forms and NO chemisorbs as cationic, neutral, and anionic NO on the supported Rh catalysts (10–15). Understanding the reactivities of various adsorbates is critical in elucidating the mechanism of the reaction of NO with CO.

The reactivity of adsorbed CO and NO toward CO_2 formation depends not only on the composition and surface state of the catalyst but also the concentration of the gaseous reactants. Our recent study has shown that the exposure of preadsorbed CO to gaseous NO over reduced Rh/SiO_2 catalyst led to the desorption of linear CO and the formation of NO^- species (16, 17). The exposure of preadsorbed NO to gaseous CO resulted in the displacement of adsorbed NO^+ and chemisorption of CO as gem-dicarbonyl and linear CO on Rh^+ (16). The presence of both NO and CO is required for the formation of CO_2 at 373 K.

Little information is available on the nature and type of adsorbates and their reactivities for the formation of products during the NO–CO reaction. The objective of this paper is to investigate the dynamic nature and reactivity of infrared-active (observable) adsorbates toward CO_2 formation during the NO–CO reaction using combined *in situ* infrared (IR) spectroscopy and mass spectrometry (MS). *In situ* IR technique was used to monitor the transient response of adsorbates; MS was used to determine the response of gaseous products. The transient techniques used in this study include switching from ^{12}CO to ^{13}CO flow during steady-state NO–CO reaction and pulsing a mixture of NO and CO in a steady-state helium flow. The former technique reveals the reactivity of intermediates leading to CO_2; the latter elucidates the competitive nature of NO and CO adsorption and the sequence for the formation of adsorbates.

EXPERIMENTAL

The Rh/SiO_2 catalyst containing 4 wt% Rh was prepared by incipient wetness impregnation of large-pore silica support (Strem, 300 m^2/g) using $RhCl_3 \cdot 3H_2O$ (Alfa Chemicals) solution. The ratio of the solution to the weight of support material used is 1 cm^3 to 1 g. The catalyst was dried overnight in air at 303 K after impregnation and then reduced in flowing hydrogen at 673 K for 8 h. Pulse CO chemisorption studies at 303 K showed that the reduced

[1] Current address: Tesa Tape Inc., Charlotte, NC 28209.
[2] To whom correspondence should be addressed.
[3] Current address: United Catalysts Inc., Louisville, KY 40232.

0021-9517/95 $12.00

Rh/SiO_2 catalyst chemisorbed 55.3 μmol CO/g catalyst corresponding to a crystallite size of 63 Å (16).

An *in situ* infrared reactor cell, with CaF_2 windows, capable of operating up to 873 K and 6 MPa was used for the NO–CO reaction studies (16, 17). The catalyst was pressed into a self-supporting disk (6 mg), placed in the reactor cell, and further reduced *in situ* at 673 K for 2 h before the reaction study. The reaction mixture consisted of CO/Ar (Linde, Custom Grade), NO, He (Linde, UHP), and ^{13}CO (Isotec, 99% ^{13}C); the gas flows were controlled by mass flow meters. The effluent from the IR reactor cell was monitored continuously using a Balzers QMG 112 quadrupole mass spectrometer. The time scale on the mass spectrometer was corrected for the time lag for the gaseous species to travel through the transportation lines from the reactor to the MS ionization chamber. The change in the concentration of the gaseous species obtained from the MS thus reflects the actual change in concentration of gaseous species in the IR reactor.

The reactant mixture of CO/Ar/NO/He was passed over the catalyst at a ratio of 1/0.02/1/3.75 and a total flow rate of 46 cm^3/min. Helium, an inert gas in the reaction, was used as a carrier to keep a low concentration of the ionized species in the MS vacuum chamber for high sensitivity to reaction products. The reaction was allowed to settle to steady state before each transient experiment. After 30 min of steady-state reaction, the flow of ^{12}CO/Ar was switched to ^{13}CO flow at 0.1 MPa, without varying the total flowrate, to produce a near step change in concentration of ^{12}CO/Ar and ^{13}CO; the transient responses for $^{12}CO_2$, $^{13}CO_2$, and C-containing adsorbates were obtained. The CO contains 2.01% Ar for determining the effect of gas holdup in the reactor and gas transportation lines on the transient response of gaseous products. The change in the concentration of the ^{12}C and ^{13}C adsorbates during the switch was monitored by a Fourier transform infrared (FTIR) spectrometer with a resolution of 4 cm^{-1}. The *m/e* ratios (i.e., the amu) monitored by the MS were *m/e* = 30 for NO, *m/e* = 28 for ^{12}CO, *m/e* = 29 for ^{13}CO, *m/e* = 44 for $^{12}CO_2$, *m/e* = 45 for $^{13}CO_2$, and *m/e* = 40 for Ar. It should be noted that ^{12}CO and N_2 give the same *m/e* at 28; $^{12}CO_2$ and N_2O give the same *m/e* at 44. Since the concentration of N_2 and N_2O did not change during the ^{13}CO isotopic transient studies, the changes in *m/e* = 28 and *m/e* = 44 resulted from the variation in concentration of CO and CO_2, respectively.

NO–CO pulse reaction studies were conducted by introducing a mixture of 5 cm^3 of NO and 5 cm^3 of CO into a constant helium flow of 30 cm^3/min by a six-port chromatographic sampling valve. The effluents from the IR reactor cell were monitored using the MS. A 6-ft Porapak Q column was incorporated into the effluent line to the MS to separate $^{12}CO_2$ and N_2O products which give the same amu (*m/e*) at 44. It has been shown that the pretreatment

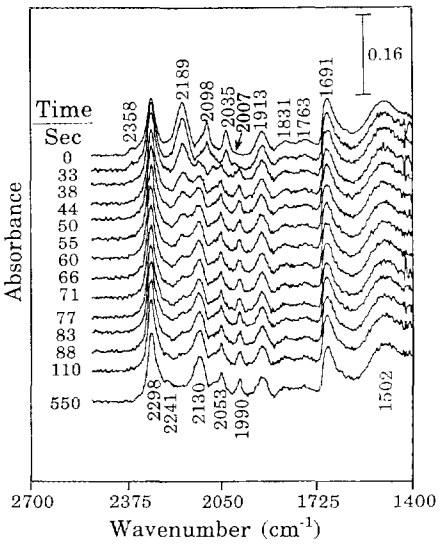

FIG. 1. IR spectra of the transient ^{13}CO isotopic switch during NO–CO reaction on Rh/SiO_2 at 523 K.

conditions affect the activity of catalysts for NO–CO reaction (6). However, in this study, the catalyst was not reduced between experiments at different temperatures in order to study the catalyst under practical conditions existing in an automotive catalytic converter where the catalyst is not periodically reduced.

RESULTS AND DISCUSSION

Steady-State Isotopic Transient NO–CO Reaction

Figure 1 shows the IR spectra obtained during the steady-state isotopic transient experiment on Rh/SiO_2 at 523 K. The initial spectrum prior to the isotopic switch shows the following bands: (i) a Si–NCO band at 2298 cm^{-1}, (ii) a Rh–NCO band at 2189 cm^{-1}, which overlaps with the P branch of the gaseous CO band (8, 16), (iii) gem-dicarbonyl bands at 2098 and 2035 cm^{-1} (6, 10–20), (iv) an NO^+ band at 1913 cm^{-1}, (v) an NO^- band at 1691 cm^{-1} denoted as low wavenumber NO^-, and (vi) a bidentate nitrato-species at 1502 cm^{-1} (10). The assignment of the bands at 1831 and 1763 cm^{-1} is not as clearly defined as that of other bands. The 1831 cm^{-1} band is in the infrared range of a neutral Rh–NO species; the 1763 cm^{-1} band has been assigned to a high wavenumber NO species (6, 16). These two bands also coincide with the infrared spectra of the dinitrosyl species which was observed on Rh^+ site on Rh/Al_2O_3 and Rh–Y zeolite (19–21). Temperature-programmed reaction studies as well as NO and CO adsorption studies showed that NO adsorbed mainly as high wavenumber $Rh–NO^-$ giving rise to an intense 1763 cm^{-1} band at temperatures below 493 K in either NO or NO–CO environment (16, 17).

A gaseous $^{12}CO_2$ band was observed at 2358 cm^{-1}. On switching from ^{12}CO to ^{13}CO flow, gaseous ^{13}CO entered the reactor about 28 s after the switch. Twenty-eight seconds is the time required for the ^{13}CO flow to travel through the transportation line from the four-port switching valve to the reactor. Infrared spectra of the adsorbate remained unchanged in the first 28 s. Switching from ^{12}CO to ^{13}CO flow resulted in the decrease in the intensity of the gaseous $^{12}CO_2$ band at 2358 cm^{-1}, a shift in the Rh–NCO band from 2189 to 2130 cm^{-1}, and a shift in the gem-dicarbonyl bands from 2098 and 2035 cm^{-1} to 2053 and 1990 cm^{-1}. The diminishing $^{12}CO_2$ intensity reflects a decrease in the $^{12}CO_2$ concentration which has also been observed in the gaseous $^{12}CO_2$ response shown in Fig. 3. The decrease in the concentration of $^{12}CO_2$ is accompanied by the increase in the concentration of $^{13}CO_2$ whose infrared band overlaps with the intense Si–NCO band. The process for replacement of ^{12}C gem-dicarbonyl by ^{13}C gem-dicarbonyl started before 33 s and completed at 66 s. During the replacement, ^{12}C gem-dicarbonyl decreased in intensity while the ^{13}C gem-dicarbonyl increased in intensity without variation of their wavenumbers. The absence of variation in wavenumber with intensity is due to the fact that both ^{12}C and ^{13}C gem-dicarbonyls are bound on isolated Rh sites (12).

A weak band at 2007 cm^{-1} appeared between 33 and 38 s; the shoulder band at 2082 cm^{-1} at 33 s emerged as a band at 38 s. These two bands, which completely disappeared at 50 s, can be assigned to the $Rh^+(^{12}CO)(^{13}CO)$ (12). Both bands have also been observed during the exposure of $Rh^+(CO)_2$ to ^{13}CO and $Rh^+(^{13}CO)_2$ to ^{12}CO and NO on Rh/SiO_2 at 373 K, which confirm the presence of $Rh^+(^{12}CO)(^{13}CO)$ (18). No change in the adsorbed nitrosyl bands was observed.

Isocyanates on Rh and SiO_2 surface, exhibiting bands at 2189 and 2298 cm^{-1}, respectively, have been observed during steady-state NO–CO reaction over Rh/SiO_2 (8, 16, 22) and NO–CO interaction over Rh/Al_2O_3 catalysts (11). It has been suggested that the NCO species is initially formed on the Rh surface and then migrates to the SiO_2 surface (22). Temperature-programmed reaction studies of the NO–CO reaction on Rh/SiO_2 show that the Rh–NCO species disappears at temperatures above 553 K while the Si–NCO remains on the surface even at 673 K (16, 17). The intensity of the Si–NCO band, shown in Fig. 1, slowly increased with time on stream while its wavenumber remained the same during the isotopic switch from ^{12}CO to ^{13}CO flow. Note that part of the increase in the intensity of the 2298 cm^{-1} band is due to the formation of $^{13}CO_2$. Figure 1 also shows that the time required for the shift of the Rh–$N^{12}CO$ band at 2189 cm^{-1} to Rh–$N^{13}CO$ band at 2130 cm^{-1} is more than 87 s while the time required for disappearance of the CO_2 band at 2358 cm^{-1} is only about 50 s. This result suggests that Rh–NCO does not play a significant role in the catalytic cycle of CO_2 formation from CO (8, 22). The adsorbed NCO species has been suggested to be an intermediate for N_2 formation on Cu–ZSM-5 catalyst (23). The role of NCO species in N_2 formation in the NO–CO reaction has to be determined from ^{14}NO to ^{15}NO switching experiment.

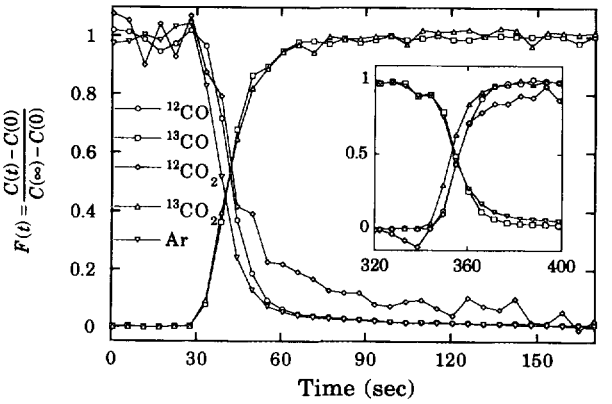

FIG. 2. MS analysis of the effluent from the reactor for the transient ^{13}CO isotopic switch during NO–CO reaction on Rh/SiO_2 at 473 K.

Steady-state NO–CO reaction and isotopic ^{13}CO transient studies were also conducted at 473 and 573 K. A comparison of the IR spectra at different temperatures showed that the intensities of the high wavenumber NO^- and gem-dicarbonyl at 473 K is slightly higher than those at 523 K, and the intensity of Rh–NCO and Si–NCO is lower than those at 523 K. The dynamic behaviors of $Rh^+(CO)_2$, $Rh^+(^{12}CO)(^{13}CO)$, and $Rh^+(^{13}CO_2)$ at 473 K resembled those at 523 K (26). The IR spectra at 573 K showed very intense gaseous CO_2 bands at 2358 and 2338 cm^{-1}, a prominent Si–NCO band at 2298 cm^{-1}, a N_2O shoulder at 2240 cm^{-1}, and a weak NO^- band at 1697 cm^{-1} (8). The absence of adsorbed CO at 573 K does not allow the determination of its dynamic behavior. The intensity of gas-phase CO_2 bands increases with temperature. The observed variation of the IR intensity of adsorbates and gaseous species with temperature is consistent with our previous temperature-programmed reaction studies (16, 17).

Figures 2, 3, and 4 show the normalized MS response of the step switch from ^{12}CO to ^{13}CO at 473, 523, and 573 K, respectively. The step transient experiments were repeated to check the reproducibility of the results. The step response is normalized using the equation

$$F(t) = \frac{C(t) - C(0)}{C(\infty) - C(0)}, \qquad [1]$$

where $F(t)$ is the normalized response, $C(0)$ is the concentration of the gaseous species at the initial steady state

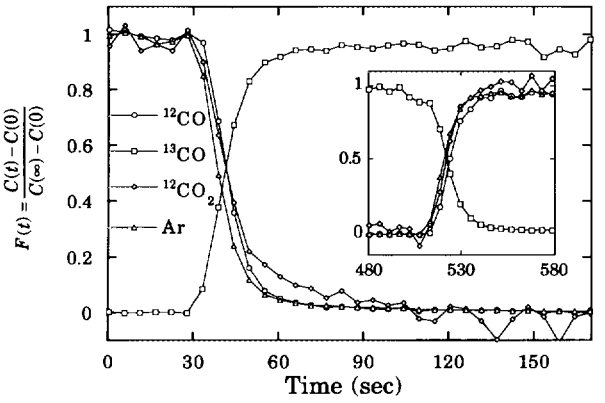

FIG. 3. MS analysis of the effluent from the reactor for the transient ^{13}CO isotopic switch during NO–CO reaction on Rh/SiO_2 at 523 K.

before the switch, and $C(\infty)$ is the concentration at the steady state after the switch was made. Figures 2, 3, and 4 show that the intersection of ^{12}CO and ^{13}CO curves occurs at $F(t) = 0.5 \pm 0.037$ during the switch from ^{12}CO flow to ^{13}CO flow and the switch from ^{13}CO back to ^{12}CO flow. The slight deviation from $F(t) = 0.5$ suggests that accurate balance of ^{12}CO and ^{13}CO flow rates was not achieved. The slight imbalance of ^{12}CO and ^{13}CO flow has less effect on the concentration of adsorbed CO during reactions such as CO hydrogenation and ethylene hydroformylation (24) where adsorbed CO is the dominant species. However, in the NO and CO reaction where adsorbed NO is more strongly bonded than adsorbed CO (6, 16), the slight imbalance in flow causes the IR intensity of adsorbed ^{13}CO to be lower than that of adsorbed ^{12}CO, as shown in Fig. 1.

Figures 2 and 3 show that the Ar response leads the ^{12}CO response and the ^{12}CO response leads the $^{12}CO_2$ response during the switch from ^{12}CO to ^{13}CO flow. The noise level in the $^{12}CO_2$ response at 473 K is higher than that for the other species monitored due to the formation of a small quantity of $^{12}CO_2$ at this temperature. The asymmetric nature of the $^{12}CO_2$ and $^{13}CO_2$ responses observed at 473 K is due to the presence of trace amounts of $^{13}CO_2$ in the ^{13}CO flow. Separate calibration studies have revealed the presence of 0.84% of $^{13}CO_2$ in ^{13}CO flow. Thus, the $^{13}CO_2$ response essentially follows the ^{13}CO response and does not provide mechanistic information. The switchback from ^{13}CO to ^{12}CO flow shown in the inset in Fig. 2 confirms the observations of the earlier switch from ^{12}CO to ^{13}CO flow. The Ar response leads ^{12}CO response and the ^{12}CO response leads the $^{12}CO_2$ response during the switchback from the ^{13}CO to ^{12}CO flow.

Figures 2 and 3 show that the ^{12}CO response, $F(t)$, drops from 1 to 0 and the ^{13}CO response rises from 0 to 1 within 33 s, which corresponds to the time required for the replacement of ^{12}C gem-dicarbonyl by ^{13}C gem-dicarbonyl shown in Fig. 1. The time for decay in the gas-phase response of the $^{12}CO_2$ took about 130 s at 473 K, 60 s at 523 K, and 33 s at 573 K to complete. An increase in temperature results in a faster $^{12}CO_2$ response. At 573 K, the $^{12}CO_2$ response leads the ^{12}CO response as shown in Fig. 4. The noise level in the $^{12}CO_2$ response is lower at 523 and 573 K than at 473 K due to the higher rate of CO_2 formation.

Table 1 lists the average residence time of adsorbed CO and intermediates for CO_2 formation calculated from the transient responses of the step switch experiments. The transient responses are affected by the flow pattern and the residence time of the flow in the reactor and transportation lines. Since Ar does not adsorb on the catalyst surface under reaction conditions, the Ar response curve represents the flow pattern and the residence time distribution of gaseous reactants flowing through the reactor and the transportation lines. The average residence time of the Ar tracer through the reactor system is calculated from the equation:

$$\tau_{Ar} = \int_0^\infty F_{Ar}(t)\, dt. \qquad [2]$$

Assuming that the flow pattern of the gaseous CO is the same as that for Ar, the average residence time of adsorbed CO is obtained from

$$\tau_{CO} = \int_0^\infty F_{CO}(t)\, dt - \tau_{Ar}. \qquad [3]$$

The shapes of the Ar curves at the three different reaction temperatures are essentially the same, indicating that flow patterns through the reactor cell and the transportation lines were not greatly affected by the IR cell temperature.

Figure 1 shows that the complete replacement of all adsorbed ^{12}CO by ^{13}CO was achieved in 33 s, which agrees with the time required for the replacement of gaseous ^{12}CO by ^{13}CO. The results suggest that a rapid exchange occurs

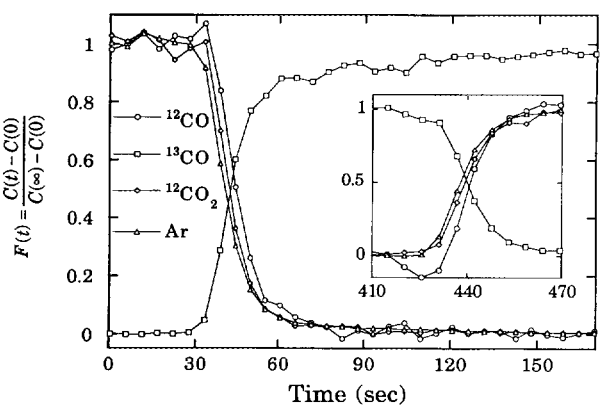

FIG. 4. MS analysis of the effluent from the reactor for the transient ^{13}CO isotopic switch during NO–CO reaction on Rh/SiO_2 at 573 K.

TABLE 1

Residence Times for CO and CO_2 Obtained during Isotopic Transient Studies on Rh/SiO_2

Temperature (K)	τ_{Ar}(s) $^{12}CO \rightarrow {}^{13}CO$	τ_{CO}(s)		τ_{CO_2}(s)	
		$^{12}CO \rightarrow {}^{13}CO$	$^{13}CO \rightarrow {}^{12}CO$	$^{12}CO \rightarrow {}^{13}CO$	$^{13}CO \rightarrow {}^{12}CO$
473	46.91	2.89	2.82	8.18	12.22
523	46.14	2.84	3.79	1.46	—[a]
573	48.59	3.70	2.00	−2.74	−0.40

[a] τ_{CO_2} could not be calculated due to an imperfect switch from ^{13}CO to ^{12}CO flow.

between gaseous CO and adsorbed CO. Gaseous ^{12}CO response may be used to represent adsorbed ^{12}CO response at 473 and 523 K. As a result, the average residence time of intermediates, τ_{CO_2}, for the CO_2 formation from adsorbed CO can be estimated from

$$\tau_{CO_2} = \int_0^\infty [F_{CO_2}(t) - F_{CO}(t)]\, dt. \qquad [4]$$

It should be noted that infrared spectra of adsorbed CO were not observed at 573 K. $F_{CO}(t)$ at 573 K represents the response of unreacted CO. The negative value obtained for τ_{CO_2} indicates that the residence time of intermediates leading to CO_2 is smaller than that for unreacted CO. Figures 2–4 show that switching from ^{13}CO to ^{12}CO was far from perfect, producing a dip in the $^{12}CO_2$ response at 473 and 523 K and a dip in the ^{12}CO response at 573 K. Hence, switching from ^{12}CO to ^{13}CO produces more accurate values of τ_{CO} and τ_{CO_2} than switching from ^{13}CO to ^{12}CO.

The rate of NO conversion and TOF at different temperatures are listed in Table 2. The TOF is defined as the number of moles of NO converted per second mole of Rh surface atom. Note that the exact nature of Rh sites for NO decomposition and CO_2 formation remains unclear. In this study, the number of Rh surface atoms was estimated by both CO chemisorption at 303 K and the infrared intensity of adsorbed NO and CO at reaction temperature.

The major CO species observed is gem-dicarbonyl; the dominant NO species is NO^- during steady-state isotopic and pulsing studies at 473 and 523 K. The amount of adsorbed NO and CO during reaction can be estimated using their integrated infrared intensities and the integrated absorption coefficient. The integrated absorption coefficient, $\bar{A}_{CO}$, for CO can be determined from the relation (25)

$$\bar{A}_{CO_g} = \frac{1}{\bar{C}_{CO}} \int_{\upsilon_l}^{\upsilon_u} A(\upsilon)\, d\upsilon, \qquad [5]$$

where $\bar{C}_{CO}$ is the moles of CO chemisorbed/cross-sectional area of the catalyst disk; $\upsilon_u = 2100\ cm^{-1}$, the upper wavenumber bound of the absorption band of gem-dicarbonyl; and $\upsilon_l = 2012\ cm^{-1}$, the lower bound of the absorption band of gem-dicarbonyl. The integrated absorption coefficients were found to be 10.8 cm/μmol for the gem-dicarbonyl and 9.9 cm/μmol for the NO^- species (26). Assuming that $\bar{A}_{CO}$ is independent of coverage and temperature, the concentration of CO can be determined from the following relation (27):

TABLE 2

Conversion and Selectivity Data Obtained during Isotopic Transient and NO–CO Pulses on Rh/SiO_2

Temp. (K)	Rate of NO conversion						Pulse study (%)	Selectivity[c]	
	(μmol/g cat · sec)	TOF[a] (s^{-1})	n_{CO} (μmol/g cat)	n_{NO} (μmol/g cat)	TOF[b] (s^{-1})	(%)		N_2O	N_2
473	105.5	1.91	76.74	37.40	0.92	11.6	12.3	3.7	96.3
523	136.4	2.47	11.88	26.17	3.58	15.0	16.2	16.2	83.8
573	572.8	10.35	—[d]	—[d]	—	63.0	95.6	0	99.5

[a] Estimated from the number of surface Rh atoms that chemisorb CO at 303 K.
[b] Estimated from the intensity of gem-dicarbonyl CO and adsorbed NO under reaction conditions.
[c] Selectivity for product i = rate of formation of product i divided by the rate of overall product formation.
[d] n_{CO} and n_{NO} could not be calculated due to absence of adsorbed CO and NO at 573 K.

$$n_{CO} = \frac{a_{CO}A_c}{m\bar{A}_{CO}}, \quad [6]$$

where n_{CO} is the number of adsorbed CO per gram of catalyst, a_{CO} is the area under the IR absorbance peak of adsorbed CO, A_c is the cross-sectional area of the catalyst disk, m is the mass of the catalyst disk, and $\bar{A}_{CO}$ is the integrated absorption coefficient of gem-dicarbonyl.

The turnover frequency (TOF) values calculated from the two different methods are found to be in the same order of magnitude. The difference in the TOF values is a result of difference in estimation of the number of Rh surface atoms from these different methods. It should be noted that CO was adsorbed as linear and bridged CO at 303 K while gem-dicarbonyl CO was adsorbed with NO under reaction conditions at 473 K and 523 K. The values for TOF obtained in this study are also in the same order of magnitude as TOF values reported in earlier studies on Rh single crystals and on a low-loading Rh/Al_2O_3 (3, 7, 9, 28, 29). The TOF calculated in this study is, however, higher than the TOF obtained over a 4.6% Rh/SiO_2 catalyst (6). The uncertainty in the estimation of the number of Rh surface atoms results in a doubtful value for TOF.

Biloen *et al.* have shown that for an irreversible surface reaction step with a single pool of surface intermediates, the surface coverage of intermediates leading to a product i can be calculated from

$$\theta_i = \mathrm{TOF}_i \cdot \tau_i, \quad [7]$$

where θ_i is defined as the surface coverage of all intermediate species that will eventually be incorporated into product i (30). The TOF listed in Table 2 appears to be overestimated, resulting in a value for θ_{CO_2} significantly greater than 1. The high value of θ_{CO_2} suggests the possibility of underestimation of the number of Rh surface sites for the reaction and the invalidity of the assumption of an irreversible step with a single pool. Both NO and CO are known to induce surface restructuring to various extents at different temperatures. Exposure of a Rh/SiO_2 surface to a mixture of 5% NO and 5% CO at 573 K results in disruption of Rh on SiO_2 surface and the formation of highly dispersed Rh (31, 32). Disruption of the Rh crystallite would yield more Rh surface atoms than those estimated from CO chemisorption at 303 K. The use of IR absorbance intensity of NO^- and gem-dicarbonyl to calculate the number of surface atoms under reaction conditions suffers from the uncertainty of the assumption that the integrated absorption coefficient is independent of reaction conditions. This approach accounts only for those surface atoms that adsorb IR-observable NO and CO. The Rh atoms adsorbing NCO and other IR-inactive adsorbates are not included in the estimation of Rh surface atoms. A more accurate approach for characterization of catalyst surface under reaction conditions remains to be developed.

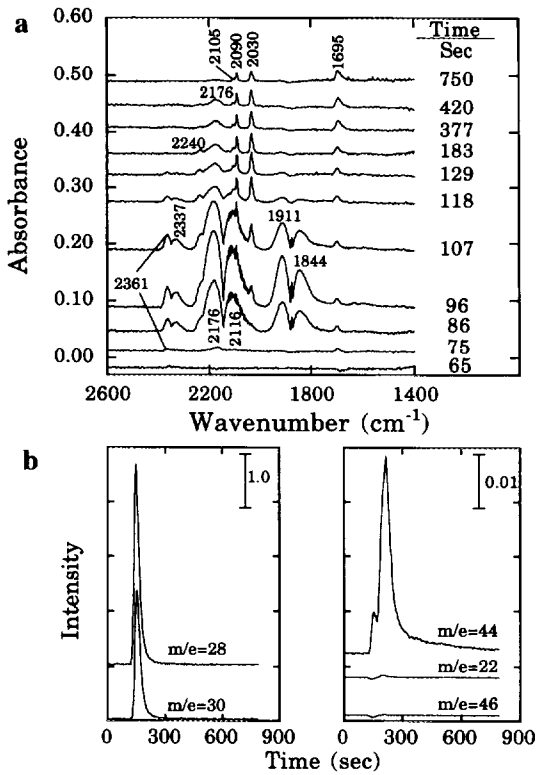

FIG. 5. (a). IR spectra of the transient NO–CO pulse at 473 K. (b). MS analysis of the effluent from the reactor for (a).

NO–CO Pulse Transient Studies

NO–CO pulse transients were conducted to study the competitive adsorption of NO and CO and to examine the various adsorbates involved in the reaction of NO and CO toward CO_2 formation. The catalyst was reduced at 673 K for 2 h prior to the pulse studies. The addition of a Porapak Q column to the effluent line of the IR cell results in the development of a small back-pressure of 0.01 MPa in He flow to the reactor. Figure 5a shows the IR spectra of the adsorbates during a pulse of 10 cm^3 of NO and CO (ratio of 1/1) mixture into a helium flow at 473 K. The IR spectra show that gaseous NO (exhibiting bands at 1844 and 1911 cm^{-1}) and gaseous CO (showing bands at 2116 and 2176 cm^{-1}) enter the reactor at about 75 s after the pulse injection of NO and CO and completely leave the reactor at about 129 s.

Upon admission of the NO–CO pulse to the IR cell, a weak CO_2 band at 2361 cm^{-1}, an NO^- band at 1695 cm^{-1}, and a Rh–NCO band at 2176 cm^{-1} were observed at about 75 s. The Rh–NCO band slowly grows in intensity to a maximum at 118 s and then decreases in intensity with

further increase in time. The Rh–NCO species has been suggested to be formed by the reaction of gaseous or adsorbed CO with adsorbed nitrogen produced from the dissociation of adsorbed NO (11, 22). The slow formation of the Rh–NCO band and the slow disappearance of the NO^- species suggests that the dissociation of NO may be a slow step at 473 K.

N_2O bands at 2240 and 2205 cm^{-1} appeared approximatley 10 s after the Rh–NCO bands are formed. About 10 s later the gem-dicarbonyl bands emerged. The intensity of the gem-dicarbonyl bands increases in the presence of gaseous CO and NO. The absence of gas-phase CO and NO causes a decrease in the gaseous CO_2, N_2O, and gem-dicarbonyl bands. The absence of change in IR intensity of OH and H_2O regions indicates that the formation of $Rh^+(CO)_2$ does not involve the OH group or the H_2O of the support. OH and H_2O have been found to participate in the formation of $Rh^+(CO)_2$ from adsorption of CO on supported Rh catalysts at 300 K (12, 14, 33–35). It is important to note that the high wavenumber NO^- at 1763 cm^{-1}, the NO^+ species at 1913 cm^{-1}, and the bidentate nitrato-species at 1502 cm^{-1}, which were previously observed during the steady-state NO and CO reaction shown in Fig. 1, are absent during NO–CO pulse studies. These species appear to form only when the catalyst surface is exposed to a steady-state flow of NO and CO. The absence of these species during the NO–CO pulse studies could be due to the slow formation of these species on the surface.

The gaseous response for *m/e* ratios corresponding to CO and N_2 (*m/e* = 28), NO (*m/e* = 30), CO_2 and N_2O (*m/e* = 44), and NO_2 (*m/e* = 46) were monitored by the MS as shown in Fig. 5b. Separation of the CO and N_2 peaks was not achieved by the addition of the Porapak Q column. However, N_2O and CO_2 peaks were separated by the column. The first *m/e* = 44 peak represents the N_2O response and the second *m/e* = 44 peak represents the CO_2 response. The secondary peak for CO_2 (*m/e* = 22), which appeared at the same time as the second *m/e* = 44 peak, was also monitored during the pulse studies to further confirm the separation of N_2O and CO_2. The tailing of the MS response of CO_2 (*m/e* = 44) could be due to either the slow conversion of gem-dicarbonyl to small amounts of CO_2 or the retention of CO_2 by the column in the effluent line to the MS. Results obtained without the column in the effluent line show that the CO_2 response closely follows that of the gaseous NO and CO response and the tailing in the CO_2 response is less than that for the CO_2 response with a column in the effluent line.

The conversion of NO was calculated as the ratio of amount of NO reacted to the amount of NO in the feed stream before reaction (bypass) as shown in Table 2. The values for conversion obtained from the pulse studies agree very well with the values obtained from the isotopic transient experiments except at 573 K. The lower conversion

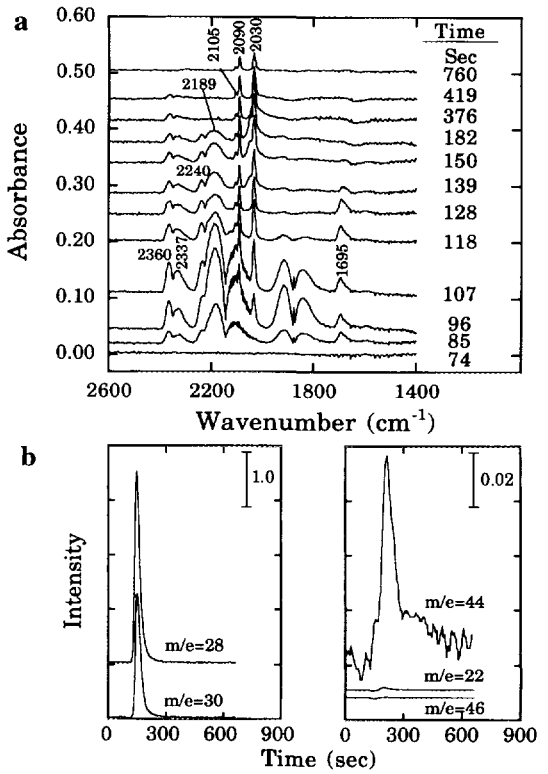

FIG. 6. (a). IR spectra of the transient NO–CO pulse at 523 K. (b). MS analysis of the effluent from the reactor for (a).

value obtained at 573 K during the isotopic transient experiments could be due to a decrease in catalyst activity on prolonged exposure of the catalyst to steady-state NO–CO flow. The selectivity toward N_2O and N_2 products were estimated as the ratio of the rate of formation of N_2O (or N_2) to the rate of overall product formation. N_2O was the major by-product in the lower temperature range of 473–523 K with a selectivity of 16% at 523 K while NO_2 was the only by-product at 573 K with a selectivity of 0.5% during the NO–CO pulse transient studies.

Figure 6a shows the IR spectra of adsorbed species during the NO–CO pulse at 523 K. A comparison of the results with those at 473 K shows that an increase in temperature from 473 to 523 K results in the slight increase in the intensity of the gem-dicarbonyl and the NO^- species in the presence of gas-phase CO and NO. The disappearance of NO^- before that of gem-dicarbonyl indicates that the gem-dicarbonyl is more stable than adsorbed NO^- at 523 K. This is in contrast to the results obtained at 473 K.

Upon NO and CO gases leaving the reactor, the intensity of NO^- decreases while the linear CO band at 2050 cm^{-1} emerged. The increase in the intensity of linear CO is also accompanied by the decrease in the intensity of NCO species suggesting that NCO may be converted to linear CO which occupies the $Rh–NO^-$ site. Our previous study

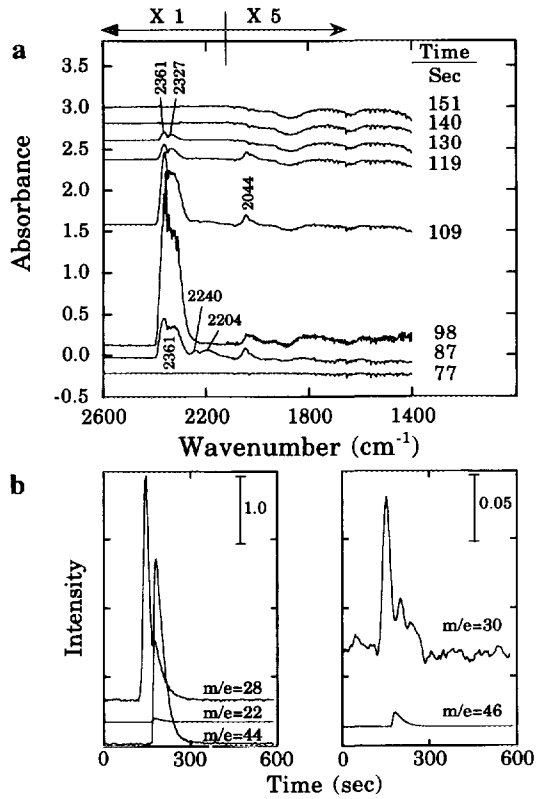

FIG. 7. (a). IR spectra of the transient NO–CO pulse at 573 K. (b). MS analysis of the effluent from the reactor for (a).

has shown that NO^- adsorbs on the reduced Rh sites where linear CO chemisorbs (16, 17). The Rh–NCO species decomposes at a higher rate at 523 K than at 473 K. The N_2O bands disappear at about the same time as that at 473 K. The slower disappearance of the CO_2 bands and a higher rate of decrease of the gem-dicarbonyl at 523 K than at 473 K suggests a higher conversion of gem-dicarbonyl to CO_2. The MS response of the effluent from the reactor is shown in Fig. 6b. The response for m/e = 28 and m/e = 30 corresponding to CO and NO, respectively, exhibits peaks without tailing while the product response for CO_2 (m/e = 44) shows a tailing peak during the pulse.

Figure 7a shows the IR spectra of the adsorbed species during the NO–CO pulse at 573 K. The IR spectra show a very weak linear CO band at 2044 cm^{-1}. The lack of adsorbed gem-dicarbonyl CO on the surface and the appearance of the linear CO band suggests that reductive agglomeration of the Rh surface occurs. It has been shown that reductive agglomeration of Rh occurs at temperatures exceeding 448 K in the presence of CO and at temperatures above 523 K in the presence of NO (14, 19). Although gaseous NO inhibits reductive agglomeration, the high NO conversion and rapid removal of oxygen by CO may result in the reduction of most Rh^+ sites to Rh^0 sites that chemisorb linear CO at 2044 cm^{-1}. The occurrence of reductive agglomeration is consistent with our earlier temperature-programmed reaction studies which show the presence of linear CO at 2040 cm^{-1} at temperatures above 543 K (16, 17).

The lack of intense adsorbed CO and NO bands at 573 K could be due to the high rate of conversion and pore diffusion limitations occurring at higher temperatures. The presence of pore diffusion limitations was verified by applying the extended Weisz–Prater criterion (36, 37) to the results at 573 K. The criterion used is defined as:

$$\Phi = \frac{(r_{CO})_{obs}\rho_s L^2 g(C^s)}{2D_{eA}\int_0^{C^s} g(C)\,dC} \ll 1, \qquad [8]$$

where r_{CO} (rate of CO conversion) = 572.8 μmol/g cat · s, ρ_s (bulk density of the catalyst) = 0.4 g/cm^3, L (thickness of the catalyst disk) = 0.1 cm, $D_{CO\text{-}CO_2}$ (binary diffusivity of the CO–CO_2 system) = 0.52, ε (porosity) = (pore volume) × (density) = 0.68, τ (tortuosity) = $\sqrt{3}$, D_{eA} (effective diffusivity) = $(\varepsilon/\tau)\,D_{CO\text{-}CO_2}$ = 0.20 cm^2/s, C^s (concentration of CO at the surface of the pellet, which is assumed to be the same as the concentration of CO in the bulk reactant flow) = 4.49 μmol/cm^3, and $g(C)$ (concentration dependency) = $[NO]^{-0.2}[CO]^{0.1}$ (6).

The kinetics of reaction is assumed to follow those reported for Rh/SiO_2 (6). Since the ratio of NO to CO used in this study was 1/1, the concentration of NO was the same as that of CO. Hence, $g(C)$ can be rewritten in terms of concentration of CO as $g(C) = [CO]^{-0.2}[CO]^{0.1} = [CO]^{-0.1}$. Using this value of $g(C)$ and performing the integration in relation [8], the extended Weisz–Prater criterion was rewritten as

$$\Phi = \frac{(r_{CO})_{obs}\rho_s L^2}{2.22D_{eA}[C^s]^{1.0}} \ll 1. \qquad [9]$$

It should be noted that the change in reaction order to the first order did not significantly change the value of Φ. The binary diffusivity of NO and CO against all the products diffused out of the pore, and the multicomponent diffusivities were also calculated using the method of Reid *et al.* (38). The binary diffusivity for the CO–CO_2 system was the smallest value among all the binary and multicomponent diffusivities calculated. The smallest value of the binary diffusivity was used with tortuosity and porosity of the pellet to calculate the effective diffusivity (D_{eA}) to obtain the lowest estimate for the value of Φ. The extended Weisz–Prater criterion was calculated as Φ = 1.13, suggesting the presence of pore diffusion limitations at 573 K. The Weisz–Prater criterion was also calculated at 473 and 523 K and the values obtained were 0.29 and 0.31,

respectively, suggesting that pore diffusion limitation is not significant at these temperatures. Ng *et al.* have pointed out that the rate of NO–CO reaction on supported Rh catalysts is often severely affected by pore diffusional limitations at temperatures above the light-off temperature, which is consistent with our results (9). Temperature-programmed reaction studies showed that the light-off temperature for the NO–CO reaction over Rh/SiO_2 catalyst was 553 K (16, 17).

Weak N_2O bands and strong bands associated with CO_2 and Si–NCO species were observed at 573 K. The absence of an N_2O MS response at $m/e = 44$ suggests that N_2O undergoes a fast surface reaction with CO to form N_2 and CO_2 at 573 K. ^{13}CO isotopic cycling experiments conducted over a Rh/Al_2O_3 catalyst have also shown the occurrence of the fast surface reaction between N_2O and CO to form N_2 and CO_2 at temperatures above light-off for the NO–CO reaction (39). Figure 7b shows the product response of the effluent from the IR reactor cell during NO–CO pulse studies at 573 K. CO_2 ($m/e = 44$) is the major product formed during the pulse while a small amount of NO_2 is also observed. NO conversion of 95.6% was obtained at this temperature. The noisy nature of the NO response is due to a low concentration of NO in the effluent stream.

The dominant adsorbed CO during NO–CO steady-state and pulse reaction studies, shown in Figs. 1, 5a, and 6a, at 473 and 523 K is gem-dicarbonyl. The mechanism of gem-dicarbonyl formation during NO–CO reaction may be elucidated from transient IR results. IR spectra in Fig. 1 and the transient response in Fig. 3 show that the time required for the replacement of the ^{12}C gem-dicarbonyl by ^{13}C gem-dicarbonyl and the time taken for the replacement of gaseous ^{12}CO by gaseous ^{13}CO are the same. The results suggest the occurrence of rapid exchange between gaseous CO and gem-dicarbonyl according to the relation

$$2CO_g + Rh_s^+ \Leftrightarrow Rh_s^+(CO)_2. \qquad [10]$$

Rh_s^+, the Rh cation on the surface, appears to result from the oxidation of Rh by NO dissociation or NO adsorption rather than the oxidative disruption involving the surface hydroxyl groups. This proposition is supported by the IR results of the NO–CO pulse studies which show

(i) the formation of gem-dicarbonyl after the adsorption of NO and

(ii) the absence of a change in the OH group during the formation of gem-dicarbonyl.

It should be noted that the formation of gem-dicarbonyl from adsorption of CO on Rh^+ may be more complex than written in Eq [10]. Yates *et al.* have suggested that $Rh^+(CO)_2$ is formed from the reaction $CO + Rh^+(CO) \Leftrightarrow Rh^+(CO)_2$, during the oxidative disruption of Rh crystallites (12). $Rh^+(CO)_2$ is likely to form through more than one elementary step. The observation of $Rh^+(^{12}CO)(^{13}CO)$ during the isotopic switch shown in Fig. 1 further confirms the adsorption of CO on $Rh^+(CO)$.

Solymosi *et al.* (19) have assumed that the formation of Rh^+ in the presence of NO follows steps [11] and [12]:

$$Rh_y - NO \Leftrightarrow Rh_{y-1} - NO^- + Rh^+ \qquad [11]$$

$$Rh_y - NO \Leftrightarrow Rh_{y-2} + 2Rh^+ + O^{2-} + \frac{1}{2}N_2. \qquad [12]$$

The steady-state isotopic transient study has shown that step [10] is a rapid process. Thus, the slow formation of gem-dicarbonyl during the pulse study may be attributed to the slow rate of formation of Rh^+. According to step [11], Rh^+ should be formed simultaneously with the formation of $Rh–NO^-$ on the surface. However, the formation of the $Rh–NO^-$ before the gem-dicarbonyl during NO–CO pulse studies indicates that the formation of Rh^+ is more complex than described by steps [11] and [12], which are assumed to take place on Rh/Al_2O_3 at 300 K in the presence of NO. The Rh^+ on the surface may be formed by the oxidation of Rh sites by oxygen obtained from the slow dissociation of the adsorbed NO. Rh^+ formed is then occupied by CO to form gem-dicarbonyl during NO–CO pulse studies. Under steady-state conditions, Rh^+ can also adsorb NO as $Rh^+–NO$ or possibly as $Rh^+(NO)_2$ as shown in Fig. 1. The formation of these NO species appear to be less competitive than that of gem-dicarbonyl species.

The role of gem-dicarbonyl in CO_2 formation can be revealed, in part, by transient infrared spectra of pulsing studies shown in Figs. 5 and 6. Small amounts of CO_2 were continuously produced in the absence of gaseous CO and NO while the intensity of gem-dicarbonyl diminished, indicating that this species may be an intermediate. However, CO_2 production prior to the appearance of this surface moiety indicates that the gem-dicarbonyl is not the only intermediate. The formation of CO_2 from CO may proceed according to the following scheme:

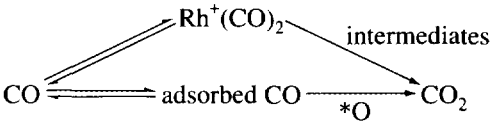

The formation of the CO_2 from gem-dicarbonyl could be due to either: (i) the disproportionation of gem-dicarbonyl CO or (ii) the reduction of Rh^+ by the oxidation of a CO ligand of $Rh^+(CO)_2[2Rh^+(CO)_2 + O^{-2} \rightarrow (Rh)_2 - CO + CO_2 + 2CO]$ (14). The absence of $(Rh)_2 - CO$ during the NO–CO pulse and isotopic transient studies suggests that the latter step did not occur.

Close examination of transient infrared spectra and CO_2 response show that about 80% of $^{12}CO_2$ initially formed followed the ^{12}CO response very closely (in Fig. 3) between 33 and 49 s during the switch from ^{12}CO to ^{13}CO. Twenty percent of the CO_2 formed between 50 and 88 s lagged significantly behind CO response. During this period, the response of gem-dicarbonyl intensity shown in Fig. 1 led that of CO_2 shown in Fig. 3. The species that leads to the lagged response of CO_2 between 50 and 88 s cannot be clearly discerned from the infrared spectra. The adsorbed species involved in the CO_2 response between 50 and 88 s could be either IR inactive or exhibit a low IR absorbance intensity. The decay of Rh–$N^{12}CO$ intensity lagged the decay of the CO_2 response between 50 and 88 s. This result suggests that Rh–$N^{12}CO$ did not directly contribute toward the response for the formation of CO_2. The two-stage behavior of the CO_2 response, where the CO_2 response initially closely follows the CO response while it lags behind the CO response after 80% of CO_2 is formed, was also observed during steady-state isotopic transient kinetic investigation of the CO–NO reaction over a commercial three-way auto catalyst at 473 K (40). The lag time for the CO_2 response decreased with increase in temperature. At 573 K, the entire CO_2 response led the CO response.

The reactivity of adsorbed CO can also be affected by the availability of adsorbed O, which is produced from NO dissociation. Pulsing studies show that the rate of disappearance of NO^- is faster than that of gem-dicarbonyl at 523 K suggesting that NO dissociates at a higher rate than at 473 K. τ for CO_2 is found to decrease drastically with increase in temperature from 473 to 573 K. At 573 K, the lower value of τ_{CO_2} than τ_{CO} indicates that adsorbed oxygen is readily available to react with adsorbed CO to form CO_2 due to the higher NO dissociation rate at this temperature. Linear CO, the only adsorbed CO observed at 573 K in this study, appears to react rapidly with the adsorbed oxygen on the surface to form CO_2.

CONCLUSIONS

The major observations that can be obtained from the steady-state isotopic transients coupled with *in situ* IR can be summarized as follows:

(1) A rapid exchange between the gaseous CO and adsorbed CO occurs on the surface.

(2) $Rh^+(^{12}CO)(^{13}CO)$ is an intermediate for the exchange between $Rh^+(^{12}CO)_2$ and gaseous ^{13}CO.

(3) The adsorbed NCO species is not directly involved in the formation of CO_2.

(4) The residence time of the intermediate for CO_2 formation decreases with an increase in temperature from 473 to 573 K.

The rapid exchange between gaseous CO and adsorbed CO during isotopic transient studies does not allow the determination of reactivity of gem-dicarbonyl toward CO_2 formation. Gem-dicarbonyl CO may be a kinetically significant species involved in the formation of CO_2. The possible overlapping of infrared spectra of adsorbates does not allow a clear distinction on the type of IR-active adsorbates involved in the formation of CO_2 that exhibits a slow response.

Pulse transients coupled with IR is an excellent complementary technique to steady-state isotopic studies although it provides information on the reactivity of adsorbate under unsteady-state condition. Pulse study further confirms that the NCO species is not directly involved in the formation of CO_2. Under pulse conditions, Rh–NO^-, Rh–NCO, and CO_2 are formed prior to gem-dicarbonyl; CO_2 can be formed from species other than gem-dicarbonyl. Further studies are required to reveal the difference in reactivity of linear CO and gem-dicarbonyl.

ACKNOWLEDGMENTS

R.K. and M.W.B. are grateful for the financial support from the Department of Chemical Engineering, The University of Akron. We acknowledge Dr. R. Dumpelmann's (Macquire University, Sydney, Australia) suggestion to monitor m/e = 22 for CO_2 to separate the contributions of CO_2 and N_2O to the m/e = 44 response.

REFRENCES

1. Armor, J. N., and Li, Y., Preprints of NO_x Reduction Symposium, Division of Petroleum Chemistry, Inc. p. 14. Am. Chem. Soc., Washington, DC, 1994.
2. Taylor, K. C., *Catal. Rev. Sci. Eng.* **35**(4), 457 (1993).
3. Oh, S. H., Fisher, G. B., Carpenter, J. E., and Goodman, D. W., *J. Catal.* **100,** 360 (1986).
4. Schwartz, S. B., Fisher, G. B., and Schmidt, L. D., *J. Phys. Chem.* **92,** 389 (1988).
5. Cho, B. K., Shanks, B. H., and Bailey, J. E., *J. Catal.* **115,** 486 (1989).
6. Hecker, W. C., and Bell, A. T., *J. Catal.* **84,** 200 (1983).
7. Belton, D. N., and Schmieg, S. J., *J. Catal.* **144,** 9 (1993).
8. Srinivas, G., Chuang, S. S. C., and Debnath, S., *In* "Automotive Emission Catalysis" (J. N. Armor and R. M. Heck, Eds.), ACS Symposium Series, p. 167. Am. Chem. Soc., Washington, DC, 1994.
9. Ng, K. Y. S., Belton, D. N., Schmieg, S. J., and Fisher, G. B., *J. Catal.* **146,** 394 (1994).
10. Arai, H., and Tominaga, H., *J. Catal.* **43,** 131 (1976).
11. Solymosi, F., and Sarkany, J., *Appl. Surf. Sci.* **3,** 68 (1979).
12. Yates, J. T., Jr., Duncan, T. M., Worley, S. D., and Vaughan, R. W., *J. Chem. Phys.* **70,** 1219 (1979).
13. Worley, S. D., Rice, C. A., Mattson, G. A., Curtis, C. W., Guinn, J. A., and Tarrer, A. A., *J. Phys. Chem.* **86,** 2714 (1982).
14. Solymosi, F., and Pazstor, M., *J. Phys. Chem.* **89,** 4789 (1985).
15. Chuang, S. S. C., and Pien, S. I., *J. Catal.* **135,** 618 (1992).
16. Srinivas, G., Chuang, S. S. C., and Debnath, S., *J. Catal.* **148,** 748 (1994).
17. Chuang, S. S. C., Krishnamurthy, R., and Srinivas, G., *in* "Symposium on NO_x Reduction" (U. Ozkan, S. Agarwal, and G. Marcelin Eds.), ACS Symposium Series, p. 183. Am. Chem. Soc., Washington, DC, 1994.

18. Chuang, S. S. C., Krishnamurthy, R., and Tan, C. D., *Colloids Surf A: Physicochem. Eng. Aspects,* in press (1995).
19. Solymosi, F., Bansagi, T., and Novak, E., *J. Catal.* **112,** 183 (1988).
20. Hyde, E. A., Rudham, R., and Rochester, C. H., *J. Chem. Soc. Faraday. Trans. 1* **80,** 531 (1984).
21. Iizuka, T., and Lunsford, J. H., *J. Mol. Catal.* **8,** 391 (1980).
22. Hecker, W. C., and Bell, A. T., *J. Catal.* **85,** 389 (1984).
23. Iwamoto, M. H., Yahiro, S., Shundo, Y., and Yu-u, N., *Shokubai Mizuno* **33,** 430 (1990).
24. Balakos, M. W., Ph.D. dissertation, The University of Akron, Akron, OH, 1994.
25. Winslow, P., and Bell, A. T., *J. Catal.* **86,** 158 (1984).
26. Krishnamurthy, R., Ph.D. dissertation, The University of Akron, Akron, OH, 1995.
27. Rasband, P. B., and Hecker, W. C., *J. Catal.* **139,** 551 (1993).
28. Oh, S. E., and Eickel, C. C., *J. Catal.* **128,** 526 (1991).
29. Peden, C. H. F., Goodman, D. W., Blair, D. S., Berlowitz, P. J., Fisher, G. B., and Oh, S. H., *J. Phys. Chem.* **92,** 1563 (1988).
30. Biloen, P., Helle, J. N., van Den Berg, F. G. A., and Sachtler, W. M. H., *J. Catal.* **81,** 450 (1983).
31. Krause, K. R., and Schmidt, L. D., *J. Catal.* **140,** 424 (1993).
32. Schwartz, J. M., and Schmidt, L. D., *J. Catal.* **148,** 22 (1994).
33. Basu, P., Panayotov, D., and Yates, J. T. Jr., *J. Phys. Chem.* **91,** 3133 (1987).
34. van't Blik, H. F. J., van Zon, J. B. A. D., Huizinga, T., Vis, J. C., Koningsberger, D. C., and Prins, R., *J. Phys. Chem.* **87,** 2264 (1983).
35. Chuang, S. S. C., and Debnath, S., *J. Mol. Catal.* **79,** 323 (1993).
36. Weisz, P. B., and Prater, C. D., *in* "Advances in Catalysis" (W. G. Frankenburg, V. I. Komarewsky, and E. K. Rideal, Eds.), Vol. 6, p. 143. Academic Press, New York, 1954.
37. Froment, G. F., and Biscoff, K. B., "Chemical Reactor Analysis and Design," p. 167. Wiley, New York, 1990.
38. Reid, R. C., Prausnitz, J. M., and Poling, B. E., "The Properties of Gases and Liquids," p. 587. McGraw–Hill, New York, 1987.
39. Cho, B. K., *J. Catal.* **148,** 697 (1994).
40. Oukaci, R., Blackmond, D. G., Goodwin, J. G. Jr., and Gallaher, G. R., *in* "Catalytic Control of Air Pollution" (R. G. Silver, J. E. Sawyer, and J. C. Summers, Eds.), ACS Symposium Series, Vol. 495, p. 61. Am. Chem. Soc., Washington, DC, 1992.